

# **Correcting 19th and 20th century sea surface temperatures improves simulations of Atlantic hurricane activity**

Duo Chan<sup>1\*</sup>, Gabriel A. Vecchi<sup>2</sup>, Wenchang Yang<sup>2</sup>, and Peter Huybers<sup>1</sup>

duochan@g.harvard.edu

<sup>1</sup>*Department of Earth and Planetary Sciences, Harvard University USA*

<sup>2</sup>*Department of Geosciences, Princeton University USA*

**Changes in the statistics of North Atlantic hurricanes are known to depend upon the pattern of tropical sea surface temperatures (SSTs). Dynamical and statistical models are key tools to predict future hurricane activity, with our confidence in this application rooted in the models' ability to skillfully reproduce hurricane variations over the past 30-40 years, when satellite data allows accurate reconstruction of observed ocean temperature variations. Extending the evaluation of simulations forced with historical SSTs against hurricane activity to century scales provides a more complete assessment of predictive skill, but which is limited in part by uncertainty in historical SST estimates. Here we show that recent corrections for systematic offsets in bucket SST measurements improve model skill in recovering North Atlantic hurricane counts and lead to consistent reproducibility since the late 19th century. Changes in hurricane frequency introduced by revising historical SST data are of similar magnitude to projected changes for 2081-2100 in response to increasing greenhouse gases, highlighting the importance of accurately assessing SST patterns for purposes of both historical and future predictions.**

21 Changes in Atlantic hurricane activity in response to climate variations remain uncertain<sup>1,2</sup>  
22 but have major societal implications<sup>3,4</sup>. Available historical records show substantial multidecadal  
23 variations in Atlantic hurricane activity<sup>5</sup> that covary with SST differences between the Atlantic  
24 main development region and the remainder of the Tropics<sup>6,7</sup>. Both statistical<sup>5,6,14</sup> and dynamical  
25 models<sup>7</sup> are skillful in reproducing variations in observational estimates of hurricane frequency  
26 over recent decades. Such covariation supports an interpretation that SST variations are a proxy  
27 for variations in hurricane available potential energy associated with the temperature difference  
28 between the surface and Tropical tropopause<sup>5,8,9</sup>. When extended to cover the late 19th and the  
29 full 20th century with commonly-used reconstructions of SSTs, however, models fail to capture the  
30 amplitude of multi-decadal variations in reconstructed hurricane counts. For example, statistical  
31 models based on tropical SST differences predict hurricane activities that are weaker than observed  
32 during the late 19th century and stronger in the middle of the 20th century<sup>6,7</sup>. Similar discrepancies  
33 arise when we simulate hurricanes using a high-resolution dynamical atmospheric model<sup>10</sup> and  
34 HadISST1<sup>11</sup> historical SST estimates (Fig. 1a).

35 Discrepancies in the long-term relationship between reconstructed and modeled Atlantic hur-  
36 ricane counts may arise for a variety of reasons. Such discrepancies could reflect errors in historical  
37 hurricane reconstructions. For example, prior to the satellite era, hurricane reconstructions must  
38 be corrected for missed events, a process that is inevitably uncertain<sup>5,6</sup>. Even in the satellite era,  
39 the classification of hurricanes can be uncertain on account of errors in maximum wind speed  
40 estimates<sup>12</sup>. A framework of reproducing hurricane activity solely on the basis of historical SST  
41 variations is also suspect. For example, upper-level atmospheric conditions have the potential to

42 evolve independently of SSTs<sup>13,14</sup>. Recent simulations also indicate that hurricane frequency de-  
43 creases with increasing CO<sub>2</sub> independent of an SST influence<sup>15</sup>. An additional possibility, which  
44 is the focus here, is that errors in SST estimates corrupt past simulation skill.

45 All widely-used estimates of historical SST variability depend upon in situ observations  
46 compiled in the International Comprehensive Ocean-Atmosphere Data Set<sup>16,17</sup> (ICOADS, Fig. 2a).  
47 This data requires corrections to account for temporal and spatial inhomogeneity in measurement  
48 strategies<sup>18-20</sup>. Prior to the 1980s, data comes largely from measurements made using buckets,  
49 comprising 40% of observations between 1942-1981 and 95% of observations prior to 1942<sup>21</sup>.  
50 Bucket temperatures are estimated to be, on average, biased 0.5°C toward cooler temperatures  
51 over the early 20th century<sup>22</sup> foremost because of cooling from wind-induced evaporation<sup>20</sup>. Other  
52 biases are also present, however, such as heating of a bucket by the sun<sup>22,23</sup>, and the degree to which  
53 cooling and heating influences temperature observations depends upon the design of a bucket and  
54 measurement protocols.

55 Lack of metadata by which to make specific corrections has necessitated simplifying as-  
56 sumptions regarding the spatial and temporal structure of bucket biases. HadISST1, for example,  
57 uses globally uniform and linear weights to represent a transition from wooden buckets to less-  
58 insulated canvas buckets<sup>11</sup>. Since hurricanes and other climate phenomena are sensitive to patterns  
59 of tropical SST changes<sup>5,24,25</sup>, however, correctly diagnosing the spatio-temporal evolution of these  
60 biases could be important. A recently developed method allows for intercomparison of nearby SST  
61 measurements to identify systematic offsets among various groups of ships<sup>26</sup> and for correction of

62 regional SST biases in accord with the uneven spatial and temporal sampling of individual ship  
63 groups. These biases range between  $\pm 0.5^\circ\text{C}$  and their correction gives a more globally homoge-  
64 neous pattern of warming over the early 20th century that is in better agreement with near-shore  
65 measurements of surface atmospheric temperature<sup>27</sup>.

66 More specifically, groupwise SST corrections lead to a warming of the Tropical Atlantic, and  
67 a general cooling elsewhere in the Tropics in the late 19th century (Fig. 2c). A hurricane-permitting  
68 atmospheric model that skillfully recovers many aspects of hurricane climatology<sup>10</sup> (Fig. 2b) indi-  
69 cates that these late-19th century SST corrections substantially impact hurricane simulations across  
70 the globe (Fig. 2d).

71 Groupwise SST corrections also lead to revisions in multidecadal variations of SST differ-  
72 ences between the Atlantic main development region and the tropical average across the 19th and  
73 20th century (Fig. 3, see "relative SST index" in methods). Correction of SST data coming from  
74 Germany, Netherlands, and a group of data whose nationality is unknown and is referred to as  
75 deck number 156 makes the main development region warmer between 1880-1930. Between 1930  
76 and 1960 British and Germany SST corrections result in colder SSTs in the main development re-  
77 gion, whereas Japanese and Netherlands SST corrections give warmer SSTs over Tropical oceans  
78 and, therefore, a decrease in the relative SST difference. To quantitatively explore implications  
79 of groupwise corrections to SSTs for hurricane simulations, we correct HadISST1 for groupwise  
80 bucket offsets, referred to as HadISST1b, and perform a paired suite of hurricane permitting model  
81 simulations spanning 1871-2019 using this revised SST dataset. Our reference experiment set is,

82 on the other hand, forced with HadISST1.

83 Changes in hurricane counts between the atmospheric model experiment forced with HadISST1  
84 and with HadISST1b (Fig. 1c) are consistent with corrections in the relative SST index (Fig. 3).  
85 The HadISST1b-forced simulations yield increased Atlantic hurricane activity in the late 19th cen-  
86 tury (Fig. 1d, Fig. 2d) and decreased activity in the middle 20th century (Fig. 1c) and reproduce  
87 multi-decadal variations in better accord with the historical reconstruction (Fig. 1b). The explained  
88 variance (square of Pearson's correlation,  $r^2$ ) for 15-year running averaged counts increases sig-  
89 nificantly ( $P < 0.05$ ) from 0.21 between observations and HadISST1-based simulations to 0.44  
90 between observations and HadISST1b-based simulations (Extended Data Fig. 1). A complimen-  
91 tary statistic, the root-mean-square error (RMSE), decreases significantly ( $P < 0.05$ ) from 1.06 hurri-  
92 canes per year between observations and simulations with HadISST1 to 0.83 between observations  
93 and simulations with HadISST1b ( $P < 0.05$ ) throughout 1885-2011. Whereas the RMSE of 1.06  
94 with HadISST1 is exceptionally unlikely ( $P < 0.01$ ) to arise solely from atmospheric internal vari-  
95 ability, errors in hurricane adjustments and previously reported SST uncertainties, the RMSE of  
96 0.83 with HadISST1b ( $P = 0.1$ , Extended Data Fig. 2) is less obviously inconsistent with known  
97 errors. Improvements in model's reproduction skill are robust to how we calibrate the model or  
98 smooth time series (Table 1).

99 Hurricane simulations using HadISST1b also give greater consistency between the number  
100 of observed and simulated hurricane counts in individual active and inactive periods, especially  
101 prior to the satellite era (Fig. 1d). For the active period spanning 1885-1899, simulations using

102 HadISST1 yield, on average,  $6.8 \pm 0.5$  (2 s.d. error) hurricanes per year, an activity that is signifi-  
103 cantly less ( $P < 0.05$ ) than the value of  $8.4 \pm 1.3$  from observational estimates. Predictions using  
104 HadISST1b, however, are consistent with observations at  $8.0 \pm 0.8$  hurricanes per year. During the  
105 next active period, between 1930-1959, simulations using HadISST1 yield  $8.3 \pm 0.3$  hurricanes per  
106 year, a value that is significantly higher ( $P < 0.05$ ) than the observed value of  $6.9 \pm 0.9$  hurricanes  
107 per year, whereas simulations using HadISST1b yield a more observationally consistent  $7.6 \pm 0.4$   
108 hurricanes per year.

109 Further quantification of agreement between simulated and observed hurricanes comes from  
110 a 40-year running York regression of simulated to observed hurricane counts,  $N_s = \alpha N_o + \beta$ .  
111  $N_s$  and  $N_o$  are, respectively, unsmoothed simulated and observed Atlantic hurricane counts. If  
112 model simulations perfectly follow observational estimates,  $\alpha$  equals one. On average,  $\alpha$  is 1.18  
113 over the 20th century with HadISST1 but decreases to 0.91 with HadISST1b (Fig. 4a), indicating  
114 more consistent model simulations and observed hurricane counts after accounting for groupwise  
115 SST offsets. Moreover,  $\alpha$  is more stable using HadISST1b. Quantitatively, the variation of  $\alpha$   
116 across years is 0.33 (1 s.d.) with HadISST1 and decreases to 0.16 with HadISST1b. Specifically,  
117 simulations with HadISST1b not exhibiting a peak of 1.85 in the 1920s that appears when using  
118 HadISST1 (Fig. 4a-b). The peak comes from a rapid increase in simulated hurricane counts be-  
119 tween 1920 to 1940 (Fig. 1a) that is moderated when forcing the model with HadISST1b (Fig. 1b).  
120 The rapid increase in HadISST1-based simulations involves biases in Deutsche Seewarte Marine  
121 data over the Atlantic main development region and the Japanese Kobe Collection over the Pa-  
122 cific (Fig. 3). Whereas German temperatures have an offset becoming  $0.33^\circ\text{C}$  warmer from 1920

123 to 1941, the Japanese temperatures involve a  $0.35^{\circ}\text{C}$  drop in the 1930s because of a truncation  
124 error<sup>26</sup>. As a result, the relative SST index experiences an artificial increase from 1920-1940 in  
125 ICOADS that underlies all major historical SST estimates, including HadISST1. Correcting for  
126 the national offsets decreases  $\alpha$  to 0.82 with HadISST1b (Fig. 4c).

127       Groupwise bucket SST corrections significantly improve simulated decadal variability of  
128 North Atlantic hurricane counts. There still appears scope for further reducing discrepancies be-  
129 tween observed and model-reproduced hurricane counts, including those spanning the transition to  
130 the satellite era in the early 1980s, through further improving the accuracy of historical SST data  
131 in two respects. First, engine-room-intake measurements of SST, which are more prevalent in the  
132 second half of the 20th century, are potentially subject to systematic biases associated with changes  
133 in depth of sampling, engine room design, and conversion to hull-mounted sensors<sup>18</sup>. Groupwise  
134 offsets have, however, not yet been developed for engine-room-intake measurements. Second, SST  
135 biases associated with individual ships may also contribute substantial uncertainty to regional SST  
136 patterns<sup>28,29</sup>. That is, offsets in ICOADSb are estimated and corrected after averaging ships com-  
137 ing from the same nation and data-collecting groups<sup>27</sup>, but ships within the same group may have  
138 distinct SST biases that depend on sampling characteristics or ship design.

139       Further reduction in discrepancies could also come from improving historical hurricane re-  
140 constructions or climate models. For example, reconstructions of historical hurricane counts could  
141 be further improved as more historical ship logs are rescued<sup>5,17</sup>. It would also be useful to estimate  
142 uncertainties in the HURDAT2 dataset associated, for example, with classification errors arising

143 from uncertainties in wind speed estimates<sup>12</sup>. Climate models could be further improved through  
144 better resolving the structure of hurricanes and large-scale climate processes that influence hurri-  
145 cane activity and more fully incorporating relevant physical processes and environmental factors<sup>15</sup>.

146 Our major finding is that biases in historical SST patterns are a dominant limiting factor in the  
147 ability of models to recover historical Atlantic hurricane counts at decadal timescales. The more  
148 stable relationship between observed and simulated hurricane activity found using HadISST1b  
149 supports the feasibility of accurate predictions of future hurricane activity based upon evolving  
150 SST patterns<sup>30–33</sup>. More importantly, revisions to historical bucket SSTs lead to an 18% increase in  
151 hurricane activity between 1885–1920 in the North Atlantic (Fig. 2d). This change is larger in mag-  
152 nitude than the multi-model expected decrease in hurricane frequency of 3% in the North Atlantic  
153 simulated in response to projected 21st century warming in the RCP4.5 scenario<sup>34</sup> (Extended Data  
154 Fig. 3) and of comparable magnitude to the simulated 24% reduction in the Northwest Pacific,  
155 the region having the largest predicted changes. Such a strong historical sensitivity of hurricane  
156 statistics to regional SSTs also highlights the importance of accurately predicting patterns of future  
157 SST change for purposes of accurate hurricane projections<sup>35</sup>.

- 158 1. Knutson, T. *et al.* Tropical cyclones and climate change assessment: Part II. projected response  
160 to anthropogenic warming. *Bulletin of the American Meteorological Society* (2019).
- 161 2. Cha, E. J., Knutson, T. R., Lee, T.-C., Ying, M. & Nakaegawa, T. Third assessment on  
162 impacts of climate change on tropical cyclones in the typhoon committee region—Part II:



- 163 Future projections. *Tropical Cyclone Research and Review* (2020).
- 164 3. Pielke Jr, R. A. *et al.* Normalized hurricane damage in the united states: 1900–2005. *Natural*  
165 *Hazards Review* **9**, 29–42 (2008).
- 166 4. Emanuel, K. Global warming effects on us hurricane damage. *Weather, Climate, and Society*  
167 **3**, 261–268 (2011).
- 168 5. Vecchi, G. A. & Knutson, T. R. On estimates of historical North Atlantic tropical cyclone  
169 activity. *Journal of Climate* **21**, 3580–3600 (2008).
- 170 6. Vecchi, G. A. & Knutson, T. R. Estimating annual numbers of Atlantic hurricanes missing  
171 from the HURDAT database (1878–1965) using ship track density. *Journal of Climate* **24**,  
172 1736–1746 (2011).
- 173 7. Caron, L.-P. *et al.* How skillful are the multiannual forecasts of Atlantic hurricane activity?  
174 *Bulletin of the American Meteorological Society* **99**, 403–413 (2018).
- 175 8. Emanuel, K. A. The maximum intensity of hurricanes. *Journal of the Atmospheric Sciences*  
176 **45**, 1143–1155 (1988).
- 177 9. Sobel, A. H., Nilsson, J. & Polvani, L. M. The weak temperature gradient approximation and  
178 balanced tropical moisture waves. *Journal of the Atmospheric Sciences* **58**, 3650–3665 (2001).
- 179 10. Zhao, M., Held, I. M., Lin, S.-J. & Vecchi, G. A. Simulations of global hurricane climatol-  
180 ogy, interannual variability, and response to global warming using a 50-km resolution GCM.  
181 *Journal of Climate* **22**, 6653–6678 (2009).

- 182 11. Rayner, N. *et al.* Global analyses of sea surface temperature, sea ice, and night marine air  
183 temperature since the late nineteenth century. *Journal of Geophysical Research: Atmospheres*  
184 **108** (2003).
- 185 12. Landsea, C. W. *et al.* A reanalysis of the 1921–30 Atlantic hurricane database. *Journal of*  
186 *Climate* **25**, 865–885 (2012).
- 187 13. Emanuel, K., Solomon, S., Folini, D., Davis, S. & Cagnazzo, C. Influence of tropical  
188 tropopause layer cooling on Atlantic hurricane activity. *Journal of Climate* **26**, 2288–2301  
189 (2013).
- 190 14. Vecchi, G. A. *et al.* Multiyear predictions of North Atlantic hurricane frequency: Promise and  
191 limitations. *Journal of Climate* **26**, 5337–5357 (2013).
- 192 15. Vecchi, G. A. *et al.* Tropical cyclone sensitivities to CO<sub>2</sub> doubling: roles of atmospheric  
193 resolution, synoptic variability and background climate changes. *Climate Dynamics* **53**, 5999–  
194 6033 (2019).
- 195 16. Woodruff, S., Diaz, H., Elms, J. & Worley, S. COADS release 2 data and metadata enhance-  
196 ments for improvements of marine surface flux fields. *Physics and Chemistry of the Earth* **23**,  
197 517–526 (1998).
- 198 17. Freeman, E. *et al.* ICOADS Release 3.0: a major update to the historical marine climate  
199 record. *International Journal of Climatology* **37**, 2211–2232 (2017).
- 200 18. Kent, E. C. *et al.* A call for new approaches to quantifying biases in observations of sea surface  
201 temperature. *Bulletin of the American Meteorological Society* **98**, 1601–1616 (2017).

- 202 19. Kent, E. C. *et al.* Observing requirements for long-term climate records at the ocean surface.  
203 *Frontiers in Marine Science* **6**, 441 (2019).
- 204 20. Folland, C. & Parker, D. Correction of instrumental biases in historical sea surface temperature  
205 data. *Quarterly Journal of the Royal Meteorological Society* **121**, 319–367 (1995).
- 206 21. Kennedy, J., Rayner, N., Smith, R., Parker, D. & Saunby, M. Reassessing biases and other  
207 uncertainties in sea surface temperature observations measured in situ since 1850: 2. biases  
208 and homogenization. *Journal of Geophysical Research: Atmospheres* **116** (2011).
- 209 22. Kennedy, J., Rayner, N., Atkinson, C. & Killick, R. An ensemble data set of sea surface  
210 temperature change from 1850: The Met Office Hadley Centre HadSST. 4.0.0.0 data set.  
211 *Journal of Geophysical Research: Atmospheres* **124**, 7719–7763 (2019).
- 212 23. Carella, G. *et al.* Estimating sea surface temperature measurement methods using characteris-  
213 tic differences in the diurnal cycle. *Geophysical Research Letters* **45**, 363–371 (2018).
- 214 24. Vecchi, G. A. *et al.* Statistical–dynamical predictions of seasonal north atlantic hurricane  
215 activity. *Monthly Weather Review* **139**, 1070–1082 (2011).
- 216 25. Xie, S.-P. *et al.* Global warming pattern formation: Sea surface temperature and rainfall.  
217 *Journal of Climate* **23**, 966–986 (2010).
- 218 26. Chan, D. & Huybers, P. Systematic differences in bucket sea surface temperature measure-  
219 ments amongst nations identified using a linear-mixed-effect method. *Journal of Climate*  
220 (2019).

- 221 27. Chan, D., Kent, E. C., Berry, D. I. & Huybers, P. Correcting datasets leads to more homoge-  
222 neous early-twentieth-century sea surface warming. *Nature* **571**, 393 (2019).
- 223 28. Kent, E. & Berry, D. Assessment of the marine observing system (ASMOS): final report  
224 (2008).
- 225 29. Kennedy, J., Smith, R. & Rayner, N. Using AATSR data to assess the quality of in situ sea-  
226 surface temperature observations for climate studies. *Remote Sensing of Environment* **116**,  
227 79–92 (2012).
- 228 30. Emanuel, K., Sundararajan, R. & Williams, J. Hurricanes and global warming: Results from  
229 downscaling IPCC AR4 simulations. *Bulletin of the American Meteorological Society* **89**,  
230 347–368 (2008).
- 231 31. Mendelsohn, R., Emanuel, K., Chonabayashi, S. & Bakkensen, L. The impact of climate  
232 change on global tropical cyclone damage. *Nature Climate Change* **2**, 205–209 (2012).
- 233 32. Emanuel, K. A. Downscaling CMIP5 climate models shows increased tropical cyclone activity  
234 over the 21st century. *Proceedings of the National Academy of Sciences* **110**, 12219–12224  
235 (2013).
- 236 33. Sobel, A. H. *et al.* Tropical cyclone hazard to Mumbai in the recent historical climate. *Monthly*  
237 *Weather Review* **147**, 2355–2366 (2019).
- 238 34. Bhatia, K., Vecchi, G., Murakami, H., Underwood, S. & Kossin, J. Projected response of  
239 tropical cyclone intensity and intensification in a global climate model. *Journal of Climate* **31**,  
240 8281–8303 (2018).

- 241 35. Christensen, J. H. *et al.* Climate phenomena and their relevance for future regional climate  
242 change. In *Climate Change 2013 the Physical Science Basis: Working Group I Contribution*  
243 *to the Fifth Assessment Report of the Intergovernmental Panel on Climate Change*, 1217–1308  
244 (Cambridge University Press, 2013).
- 245 36. York, D., Evensen, N. M., Martinez, M. L. & De Basabe Delgado, J. Unified equations for the  
246 slope, intercept, and standard errors of the best straight line. *American Journal of Physics* **72**,  
247 367–375 (2004).

248 **Acknowledgements** D.C. and P.H. are funded by a grant from the Harvard Global Institute. G.A.B.  
249 and W.Y. are funded by NOAA grant NA180AR4320123 and the Carbon Mitigation Initiative at  
250 Princeton University. The simulations presented in this article were performed on computational re-  
251 sources managed and supported by Princeton Research Computing, a consortium of groups including  
252 the Princeton Institute for Computational Science and Engineering (PICSciE) and the Office of Infor-  
253 mation Technology's High Performance Computing Center and Visualization Laboratory at Princeton  
254 University. The model used in this study (HiRAM) was developed at NOAA/GFDL, and is made freely  
255 available at <https://www.gfdl.noaa.gov/hiram-quickstart/>.

256 **Author contributions** D.C., G.A.V., and P.H. conceived and designed the study. D.C. developed  
257 HadISST1b and G.A.V. and W.Y. performed HiRAM simulations. D.C. led the analysis and writing.  
258 All authors contributed to interpreting results and discussed the manuscript.

259 **Competing interests** The authors declare that they have no competing financial interests.

260 **Additional Information**

261 **Correspondence and requests for materials** should be addressed to D.C.

262 **Reprints and permissions information** is available at <http://www.nature.com/reprints>.

263

**Table 1.** Model skill in reproducing historical North Atlantic hurricane counts.

Length of smoothing window	Calibration method	$r^2$		RMSE	
		HadISST1	HadISST1b	HadISST1	HadISST1b
15	add 1.1	0.21	0.44*	1.06	0.83*
15	scale by 1.2	0.21	0.44*	1.19	0.90*
15	add 1.1; splice	0.21	0.45*	1.06	0.81*
25	add 1.1	0.21	0.38**	0.90	0.74**

264

265

Shown statistics are squared Pearson’s correlation coefficient,  $r^2$ , and root-mean-square-error,

266

RMSE, between observational and ensemble-mean of simulated hurricane counts using

267

hadISST1 and HadISST1b. We explore the sensitivity of results by performing different

268

smoothing (15-year or 25-year), different model calibrations (add model results with 1.1 or

269

scale model results by 1.2), and turning off SST corrections in the satellite era (splice, see

270

methods). Results are for 1878-2018 but where an interval equal to half that of the smoothing

271

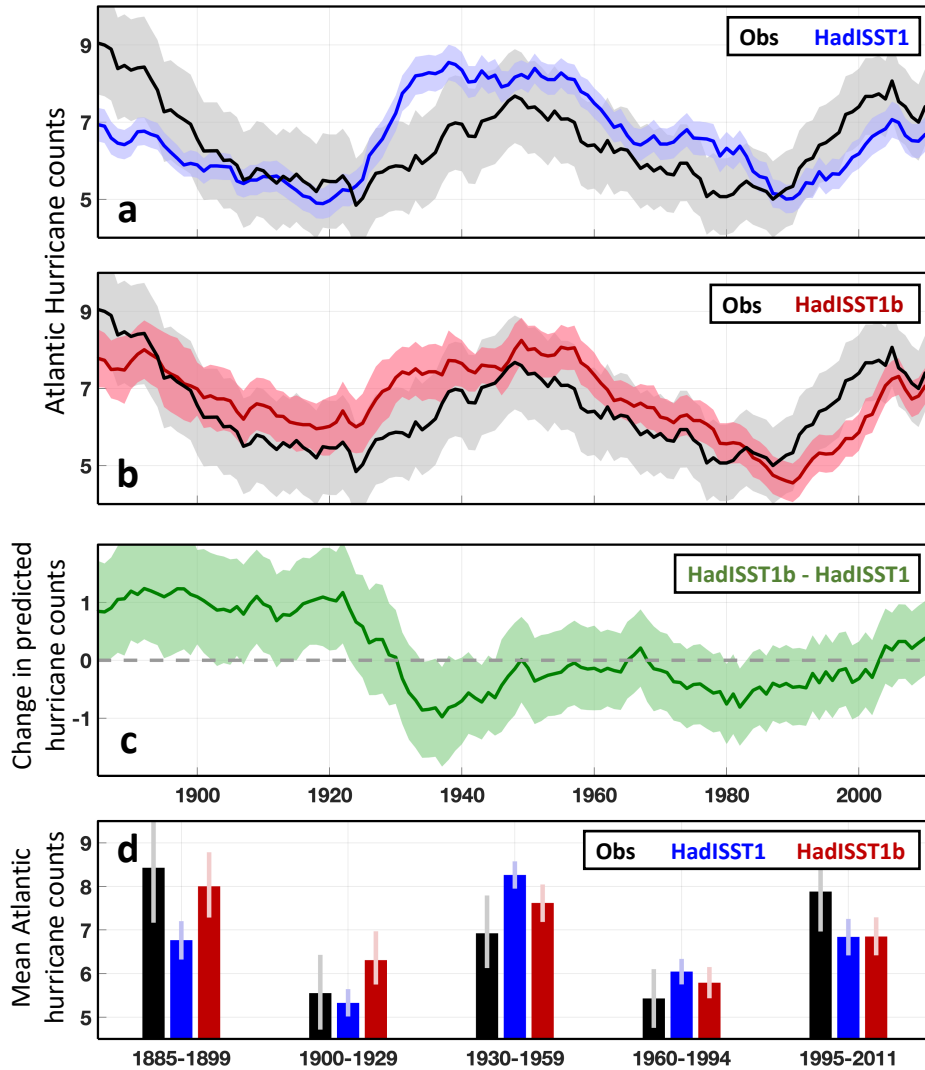
window is omitted from the beginning and end. Significant increases in  $r^2$  or decreases in

272

RMSE relative to the HadISST1 case are indicated using a “\*” ( $P < 0.05$ ) or “\*\*” ( $P < 0.1$ ).

273

Significance is evaluated using a Monte Carlo technique (see methods).



274

275

276

277

278

279

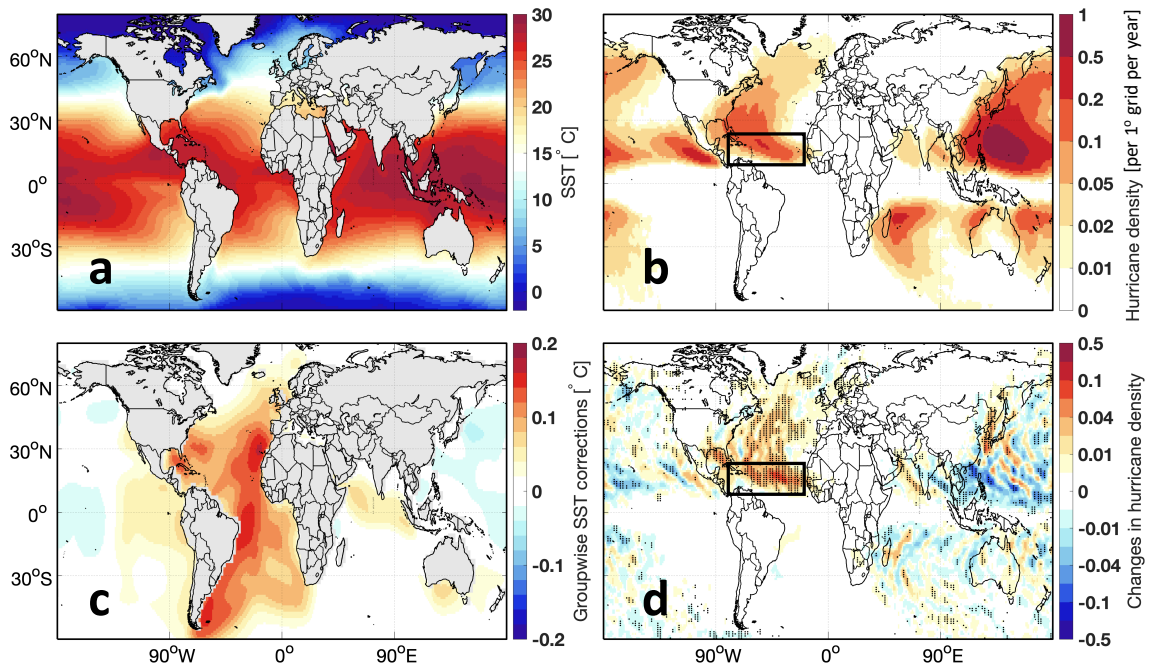
280

281

**Fig. 1. Observed and simulated Atlantic hurricane counts.** **a.** Simulations using HadISST1 give significantly lower hurricane counts in the late 19th century than observational estimates ( $P < 0.05$ ), and higher counts in the middle 20th century ( $P < 0.05$ ). **b.** Simulated and observed hurricane counts become consistent using HadISST1b, which includes corrections for groupwise SST offsets. **c.** Difference in predicted hurricane counts between simulations using HadISST1 and HadISST1b. Uncertainties are shown atmospheric for internal variability and uncertainties in hurricane adjustments added in quadrature (gray shading in panels a-b, 95%

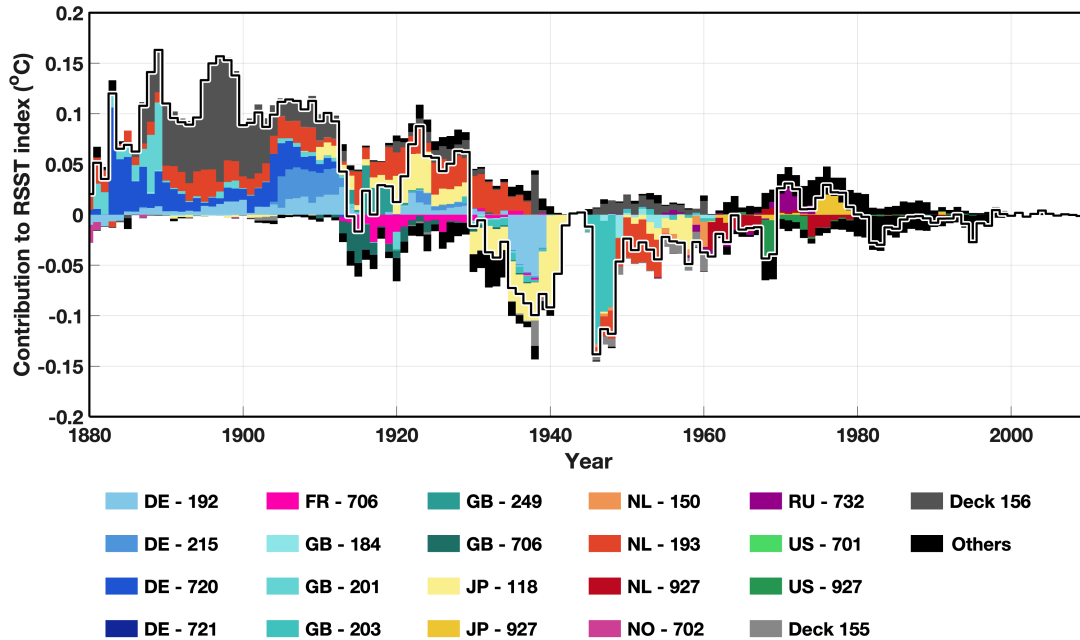


282 C.I.), atmospheric internal variability (blue shading in panel a, 95% C.I.), and atmospheric in-  
283 ternal variability and uncertainties arising from uncertain SST corrections added in quadrature  
284 (red shading, 95% C.I.). Curves in a-c are 15-year running averages with the initial (1878-  
285 1884) and final (2012-2018) 7 years truncated. **b.** Average hurricane counts over active and  
286 inactive periods where uncertainties (vertical bars, 95% C.I.) correspond to those in **a** and **b**.



287

288 **Fig. 2. Sea surface temperature and simulated hurricane counts.** **a.** Climatological SST  
 289 over 1885-1920 in HadISST1. **b.** The ensemble-mean hurricane track density averaged over  
 290 1885-1920 in simulations with HadISST1. The Atlantic main development region is high-  
 291 lighted (black box). **c.** Groupwise SST corrections averaged over 1885-1920 as incorporated  
 292 in HadISST1b, and **d.** associated ensemble-mean changes in hurricane density. Accounting  
 293 for groupwise SST offsets significantly increases hurricane density in the North Atlantic (dots,  
 294  $P < 0.05$ , two-sample t-test,  $N = 36$ ). For visualization purpose, hurricane track density on  
 295  $1^\circ$  gridding is smoothed using a nine-grid 2D convolutional smoother.



296

297

298

299

300

301

302

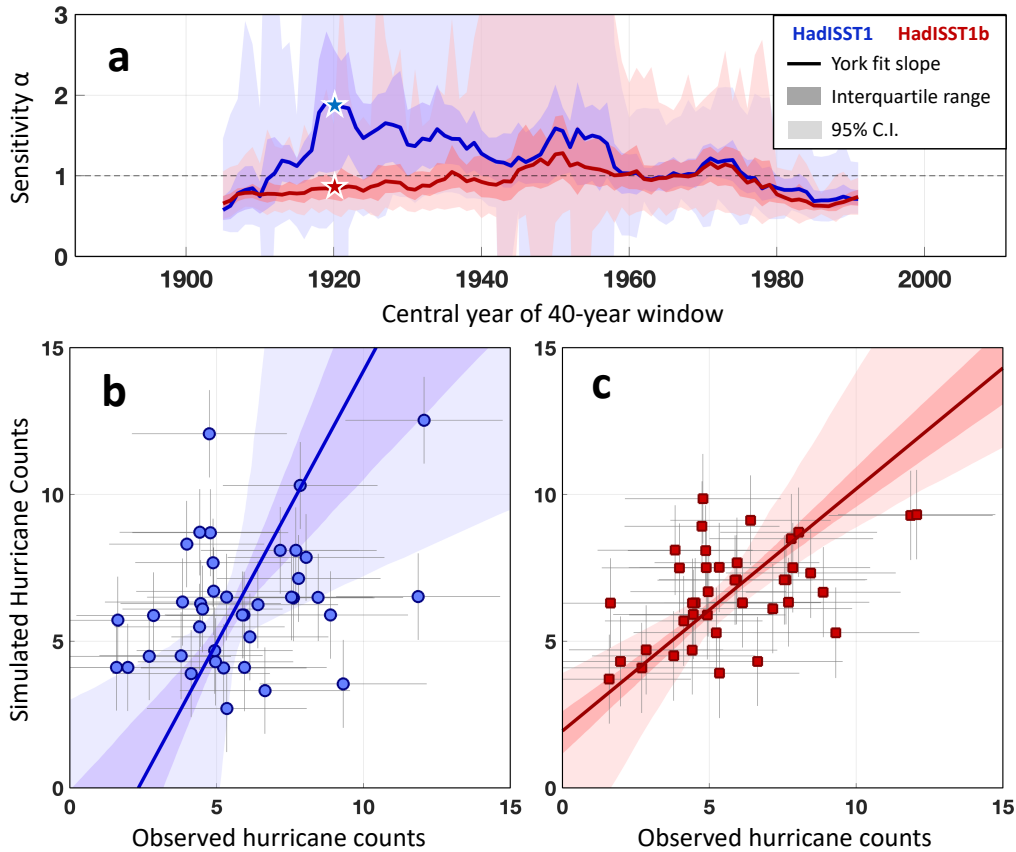
303

304

305

306

**Fig. 3. Groupwise decomposition of SST corrections in HadISST1b.** Contributions from individual groups to corrections in the relative SSTS index (black line). Relative SSTS index is a weighted difference between SST anomalies in the main development region and the entire Tropics<sup>14</sup> (also see methods). Groups are designated according to nation (two letter acronyms) and deck number, where deck is an indicator of marine data collectors in ICOADS<sup>17</sup>. Nation abbreviations are for Germany (DE), Great Britain (GB), Japan (JP), the Netherlands (NL), Russia (RU), and the United States (US). Note that the magnitude of corrections incorporated in HadISST1b trends toward lower magnitudes with time because, whereas ICOADSb is a bucket-only SST product, HadISST1b corrections are scaled by the fraction of bucket versus other measurements in individual grid boxes over time.



307

308

309

310

311

312

313

314

315

316

**Fig. 4. Regressions of simulated against observed Atlantic hurricane counts. a.** Correcting for groupwise SST offsets leads to a more stable regression slope with HadISST1b (red) than HadISST1 (blue) throughout 1885-2011. Regressions are based on unsmoothed counts using a York method<sup>36</sup> and are performed with a 40-year window that slides annually from 1885-1924 to 1972-2011. Regression slopes uncertainties are estimated using bootstrapping (dark shading is the interquartile range; light shading the 95% C.I., see methods). **b-c.** Details of York regressions using simulations with HadISST1 (**b**) and HadISST1b (**c**) over 1901-1940 (stars in **a**). York regressions account for uncertainties associated with interannual variability and hurricane count adjustments for observations (1 s.d., horizontal bars on individual markers) and

317 errors associated with interannual variability and groupwise SST corrections for simulated  
318 counts (vertical bars). Error bars are the same as in **a**.

## 319 **Methods**

320 **Observed and simulated Atlantic hurricanes:** North Atlantic hurricane observations come  
321 from the HURDAT2 dataset<sup>37</sup> (1878-2018). HURDAT2 is adjusted according to an estimate  
322 of missed hurricanes before 1965 by sampling satellite observations of hurricanes using ship  
323 tracks in the ICOADS dataset<sup>6</sup>.

324 We explore a series of SST-forced atmospheric model simulations using the NOAA-GFDL  
325 High Resolution Atmospheric Model (HiRAM) with the finite volume cubed-sphere dynam-  
326 ical core at a global 50km resolution (180x180 grid points on each of the cube faces, or  
327 C180) at 32 vertical levels<sup>10</sup>. This model has been shown to be skillful at simulating and pre-  
328 dicting many aspects of TC climatology<sup>10,38</sup> and is widely used to understand aspects of TC  
329 climatology<sup>39-43</sup>.

330 Two types of experiments are used in this study, with specified monthly-mean SST as a bottom  
331 boundary condition: 1) historical SST experiments and 2) time-slice simulations.

332 The time-varying SST-forced experiments are five-member initial- condition ensembles ini-  
333 tialized in 1871 forced with either the HadISST1 or the HadISST1b monthly SST values from  
334 1871-2019. Radiative forcing changes are prescribed from the CMIP5 historical scenario from  
335 1871-2004 and from the CMIP5 RCP4.5 scenario from 2005-2019. Simulated hurricanes are  
336 identified using a 33 m/s windspeed threshold, under which HadISST1-based HiRAM aver-  
337 ages 5.5 hurricanes per year in the North Atlantic. A value of 1.1 is added to simulated hurri-

338 canes to bring this simulated activity in line with observations of 6.6 hurricanes per year. An  
339 alternative approach of multiplying simulated Atlantic hurricane counts by 1.2 gives consistent  
340 results in terms of improved skill coming from correcting SSTs (Table 1).

341 In the “time-slice” experiments, prescribed repeating monthly SST climatology is used in or-  
342 der to assess the mean climatic impact of climatological SST changes; this method is regularly  
343 used to understand hurricane sensitivity<sup>39,43</sup>. We perform two “time-slice” experiments, each  
344 of 50-year duration, using HadISST1 SST climatology averaged over 1986-2005 and using  
345 HadISST1 SST climatology averaged over 1986-2005 plus the multi-model predicted clima-  
346 tological SST change following RCP4.5 averaged over 2081-2100<sup>43</sup> (Extended Data Fig. 3).  
347 Each experiment also includes radiative forcing relevant to each time period (fixed 1990 for  
348 the late 20th century experiment and fixed 2090 for the late 21st century experiment) following  
349 the CMIP5 historical or RCP4.5 protocol.

350 **Relative SST index:** We adopt a relative SST index (RSST) used elsewhere<sup>14</sup> to simply rep-  
351 resent the influence of variation in June-November SST to augment the more detailed results  
352 provided by the HiRAM simulations. Specifically,  $RSST = 1.388T'_{MDR} - 1.521T'_{Trop}$ , where  
353  $T'_{MDR}$  is the SST averaged over the North Atlantic main development region (20-80°W, 10-  
354 25°N, box in Fig. 2b), and  $T'_{Trop}$  is the SST averaged over Tropical oceans in general (30°S-  
355 30°N).

356 **Groupwise corrections of SSTs and mapping:** Bucket SSTs are biased both by evaporative  
357 cooling and solar heating<sup>20</sup>. The relative contributions and magnitudes of these biases de-

358 pend on bucket design and measurement protocols<sup>18,20</sup> that may differ among subsets of SST  
359 measurements. To account for systematic differences among groups of bucket SSTs, refs.<sup>26,27</sup>  
360 pair nearby measurements from distinct groups and estimate systematic offsets using a linear-  
361 mixed-effect (LME) intercomparison method. Groups are designated according to nation and  
362 deck information, where ‘deck’ previously denoted decks of punch cards in early digitization  
363 of marine observations but is used here as an additional indicator of marine data collectors.  
364 Although decks do not necessarily indicate distinct features of the data, highly statistically  
365 significant SST differences have been detected among distinct decks coming from the same  
366 nation such that their separation is appropriate for purposes of better correcting for offsets<sup>26</sup>.

367 Groupwise offsets relative to the mean of all paired SSTs are estimated using 17.8 million  
368 differenced bucket SSTs, where pairs are identified as the closest two measurements that are  
369 within 300 km and 2 days of one another. Expected differences associated with geograph-  
370 ical distributions, the seasonal cycle, and diurnal cycles are simultaneously estimated. Off-  
371 sets are then removed from individual SST measurements according to group, location, and  
372 year, yielding a gridded bucket-only SST product called ICOADSb. More details of the LME  
373 methodology are documented in ref.<sup>26</sup> and of ICOADSb in ref.<sup>27</sup>.

374 To merge the ICOADSb corrections with HadISST1, we follow five steps. (1) Groupwise  
375 SST corrections are averaged within  $2 \times 2^\circ$  grid boxes that contain bucket measurements and  
376 correspond to the HadISST1 grid. (2) Because HadISST1 uses SST measurements from a  
377 variety of methods, not only buckets, groupwise bucket corrections are multiplied by the ratio



378 of bucket to all SST measurements in individual grids for each month. Thus, all corrections  
 379 are multiplied by a fraction that is less than or equal to one. (3) Scaled correction fields are  
 380 smoothed in space using a 2D convolutional smoother with a spatial scale of 5 grid boxes. (4)  
 381 Fields are interpolated to global coverage using biharmonic spline interpolation, as encoded by  
 382 Matlab’s griddata function using the V4 method. Finally, (5), corrections in individual boxes  
 383 are tapered to zero according to an exponential decay with a 1100 km length-scale, or 10  
 384 degrees at the Equator.

385 It is worth noticing that HadISST1 makes use of satellite infrared observations since 1982<sup>11</sup>.  
 386 When calculating the ratio of bucket measurements to scale groupwise corrections, we assume  
 387 that the mass of satellite observations are five times of that from simultaneous buoy and drifter  
 388 measurements. To assess the influence of this assumption, we turn off groupwise bucket SST  
 389 corrections after 1982 and still find robust improvements in the reproduction skill of HiRAM  
 390 (Table 1 and Extended Data Fig. 4).

**Uncertainties and significance:** An error model for hurricane counts,  $H$ , can be written as,

$$H = \mathbf{F}(T) + \epsilon_i + \frac{d\mathbf{F}}{dT}(b_T + \epsilon_T) + \epsilon_o. \quad (1)$$

391  $\mathbf{F}$  is a process that maps SSTs,  $T$ , to an expected hurricane count. Both systematic SST bi-  
 392 ases,  $b_T$ , and random SST errors,  $\epsilon_T$ , introduce uncertainties in  $H$  according to  $\frac{d\mathbf{F}}{dT}$ . Hurricane  
 393 counts are also subject to atmospheric internal variability,  $\epsilon_i$ , and, for historical observations,

394 reconstruction errors associated with adjustment of missed hurricanes,  $\epsilon_o$ . This error model  
395 makes simplifying assumptions that HiRAM captures all processes relating SSTs to Atlantic  
396 hurricane counts and neglects contributions from other processes that may influence hurricane  
397 counts, such as changes in CO<sub>2</sub> concentrations<sup>15</sup>.

398 Atmospheric internal variability,  $\epsilon_i$ , is quantified using the spread of HiRAM members around  
399 the ensemble mean. The mean standard deviation of  $\epsilon_i$  over ten HiRAM simulation members  
400 (five with HadISST1 and five with HadISST1b) is 1.97 hurricanes per year. Although hurri-  
401 cane counts are integers and, therefore, should follow a Poisson distribution, the component  
402 associated with internal variability appears consistent with a Gaussian distribution (Extended  
403 Data Fig. 5) and is independent across years with lag-1 Pearson's  $r^2$  less than 0.01. Thus,  $\epsilon_i$   
404 for observed 15-year moving averaged counts becomes  $0.51 \left(\frac{1.97}{\sqrt{15}}\right)$  hurricanes per year (light  
405 gray shadings in Fig. 1a and b). For the ensemble mean of HiRAM simulations,  $\epsilon_i$  will further  
406 decrease to  $0.23\left(\frac{0.51}{\sqrt{5}}\right)$  hurricanes per year after accounting for averaging over five ensemble  
407 members.

408 Errors associated with SSTs arise both from systematic and random errors. The systematic  
409 error,  $\frac{dF}{dT}b_T$ , is approximated as equaling the groupwise corrections and are directly estimated  
410 from HiRAM simulations using the ensemble-mean difference between simulations using  
411 HadISST1 and HadISST1b (green curve in Fig. 1c). Groupwise corrections in HadISST1b  
412 decrease bias but also reveal almost an order-of-magnitude larger uncertainty in regional SST  
413 patterns than previously recognized<sup>27</sup>. Thus, it is important to also represent contributions from

414 random errors in groupwise corrections,  $\epsilon_T$ . Because of limitations in computing resources, we  
415 estimate the random error contributions using RSST, as opposed to HIRAM, through substi-  
416 tuting  $\frac{dF}{dR_{SST}}\epsilon_{RSST}$  for  $\frac{dF}{dT}\epsilon_T$  under the assumption that the RSST index sufficiently accounts for  
417 changes in hurricane counts.

418 We estimate  $\frac{dF}{dR_{SST}}$  (Extended Data Fig. 6) by regressing ensemble-average changes in hur-  
419 ricane counts between simulations with HadISST1b and HadISST1 (green curve in Fig. 1c)  
420 against changes in RSSTs between HadISST1b and HadISST1 (black curve in Fig. 3). Mean-  
421 while, we estimate  $\epsilon_{RSST}$  from a 20-member ensemble obtained by realizing errors in group-  
422 wise SST corrections in keeping with their estimated standard deviations, spatial patterns, and  
423 temporal structures<sup>26,27</sup>. The standard error in hurricane counts arising from uncertain SST  
424 corrections averages 0.23 hurricanes per year from 1885-2011 and decreases from 0.36 hur-  
425 ricanes per year in the late 19th century to less than 0.1 hurricanes per year in the satellite  
426 era. Sampling errors<sup>44</sup> and random errors associated with individual SST measurements<sup>45</sup> are  
427 omitted, but because the Atlantic main development region is well sampled since the late 19th  
428 century<sup>44</sup>, contributions from this additional uncertainty are small.

429 Observational uncertainties in hurricane counts,  $\epsilon_o$ , come from adjusting for missed storms  
430 prior to the advent of satellite observations. Adjustments are until 1965 and involve adding a  
431 correction factor to observed hurricane counts based on sampling satellite observations using  
432 ship tracks in the ICOADS dataset<sup>5</sup>. Uncertainty in the correction factor takes into account  
433 year of satellite data used, size of hurricanes, and the day of year a storm was paired with

434 observations, which yields an ensemble of 27,950 adjustment time series. Uncertainty of 15-  
435 yr smoothed hurricane counts is estimated by drawing random samples from the adjustment  
436 ensemble. Specifically, for each year, 10,000 samples are randomly drawn from 27,950 pos-  
437 sible values without replacement and under the assumption that years are independent. After  
438 smoothing the 10,000 random realizations of possible adjustments,  $\epsilon_o$  is estimated to be 0.37  
439 hurricanes per year between 1885-1964. Because of increasing numbers of ship tracks,  $\epsilon_o$  de-  
440 creases with time, from 0.44 hurricanes per year in the late 19th century to 0.23 hurricanes per  
441 year in the early 1960s.

442 When comparing difference between observations and HiRAM simulations over active and in-  
443 active periods (Fig. 1d), individual sources of errors are summed in quadrature and significance  
444 is estimated using a standard two-sample Z-test assuming errors follow Gaussian distributions.  
445 Although hurricane counts in individual years follow a Poisson distribution, errors for the en-  
446 semble mean of 15-year smoothed hurricane counts that are also subject to additional SST  
447 uncertainties are more consistent with a Gaussian distribution.

448 The significance of increases in model's reproduction skill, as measured by squared-cross cor-  
449 relation,  $r^2$ , and root-mean-square-error, RMSE, is assessed using a one-sided test against a  
450 null distribution assuming that corrections have no skill. The null distribution is realized using  
451 a Monte Carlo technique whereby mean difference between HadISST1- and HadISST1b-based  
452 simulations are permuted using 10-year blocks and then smoothed to generate randomized cor-  
453 rections. Uncertainties associated with atmospheric internal variability and hurricane counts

454 are accounted for by realizing annual noise time-series from normal distributions having stan-  
455 dard deviations equal to the estimated errors reported above. The  $r^2$  and RMSE obtained when  
456 introducing randomized corrections are calculated for each synthetic realization, and associ-  
457 ated null distributions are constructed using a total of 10,000 random realizations. The ex-  
458 pected change is negative for  $r^2$  and positive for RMSE because introducing perturbations  
459 having no skill will generally increase noise in reconstructions.

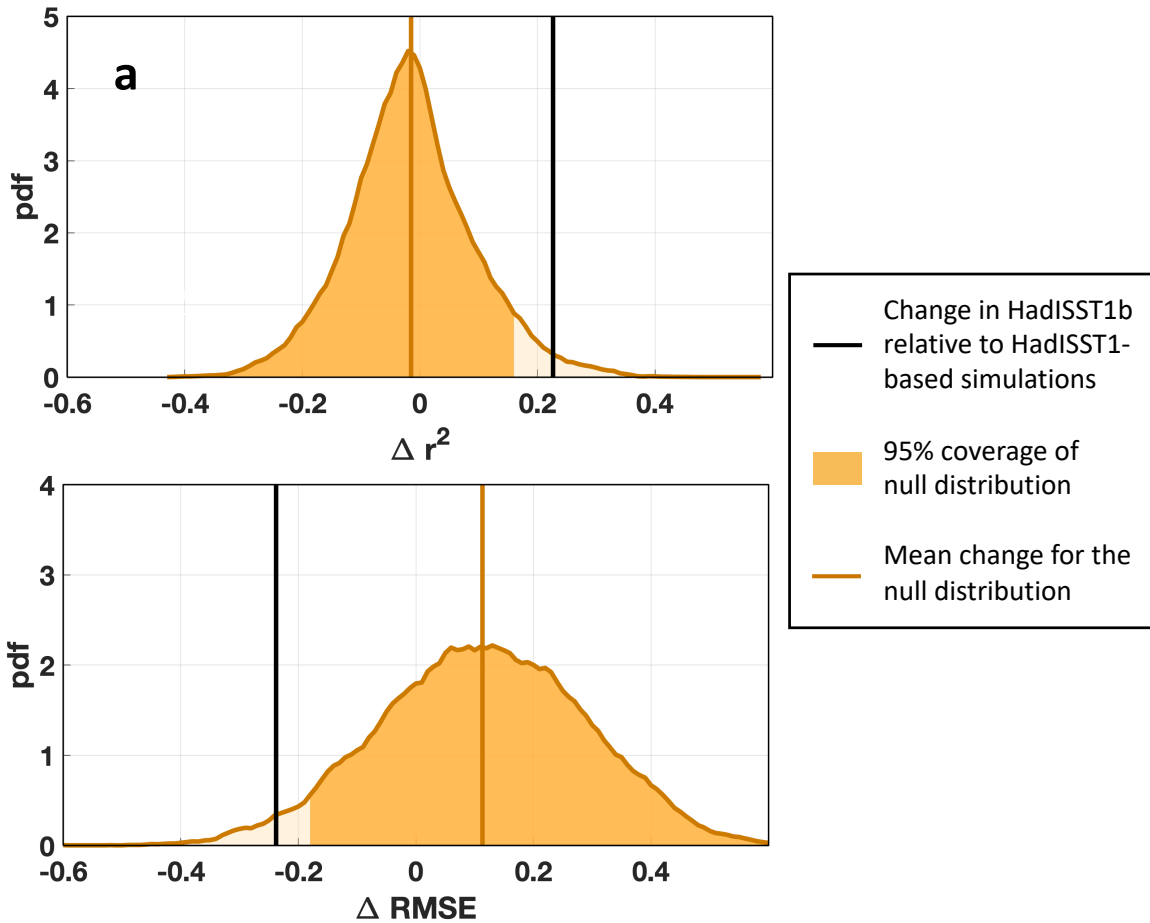
460 To estimate slopes between observed and model simulated hurricane counts (Fig. 4), we use a  
461 York regression technique<sup>36</sup> to account that both estimates are uncertain. The York regression  
462 accounts for uncertainties associated with interannual variability and hurricane count adjust-  
463 ments for observations and errors associated with interannual variability and groupwise SST  
464 corrections for simulated counts. Uncertainty of regression slopes is estimated from a 1,000-  
465 member bootstrapping ensemble that resamples 5-year blocks with replacement.

466 **Data availability:** HadISST1 is freely available at <https://www.metoffice.gov.uk/hadobs/hadisst/data/download.html>. HadISST1b and tracked hurricanes in HiRAM simulations are  
467 available from the authors upon request and will be posted on Harvard Dataverse upon publi-  
468 cation.  
469

470 **Code availability:** Code required to reproduce key results presented in this manuscript are  
471 available from the authors upon request and will be posted on Github upon publication.

- 472 37. Landsea, C. W. & Franklin, J. L. Atlantic hurricane database uncertainty and presentation of  
473 a new database format. *Monthly Weather Review* **141**, 3576–3592 (2013).
- 474 38. Zhao, M., Held, I. M. & Vecchi, G. A. Retrospective forecasts of the hurricane season using a  
475 global atmospheric model assuming persistence of SST anomalies. *Monthly Weather Review*  
476 **138**, 3858–3868 (2010).
- 477 39. Held, I. M. & Zhao, M. The response of tropical cyclone statistics to an increase in CO<sub>2</sub> with  
478 fixed sea surface temperatures. *Journal of Climate* **24**, 5353–5364 (2011).
- 479 40. Zhao, M., Held, I. M. & Lin, S.-J. Some counterintuitive dependencies of tropical cyclone  
480 frequency on parameters in a GCM. *Journal of the Atmospheric Sciences* **69**, 2272–2283  
481 (2012).
- 482 41. Merlis, T. M., Zhao, M. & Held, I. M. The sensitivity of hurricane frequency to ITCZ changes  
483 and radiatively forced warming in aquaplanet simulations. *Geophysical Research Letters* **40**,  
484 4109–4114 (2013).
- 485 42. Vecchi, G. A., Fueglistaler, S., Held, I. M., Knutson, T. R. & Zhao, M. Impacts of atmospheric  
486 temperature trends on tropical cyclone activity. *Journal of Climate* **26**, 3877–3891 (2013).
- 487 43. Knutson, T. R. *et al.* Global projections of intense tropical cyclone activity for the late twenty-  
488 first century from dynamical downscaling of CMIP5/RCP4.5 scenarios. *Journal of Climate*  
489 **28**, 7203–7224 (2015).
- 490 44. Kennedy, J., Rayner, N., Smith, R., Parker, D. & Saunby, M. Reassessing biases and other  
491 uncertainties in sea surface temperature observations measured in situ since 1850: 1. mea-

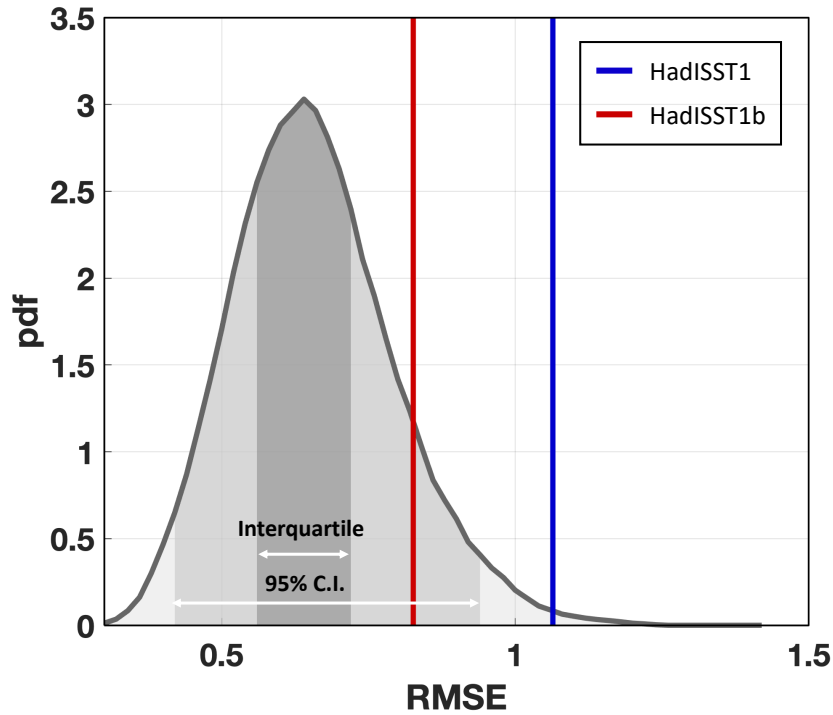
- 492 surement and sampling uncertainties. *Journal of Geophysical Research: Atmospheres* **116**  
493 (2011).
- 494 45. Kent, E. C. & Challenor, P. G. Toward estimating climatic trends in SST. Part II: Random  
495 errors. *Journal of Atmospheric and Oceanic Technology* **23**, 476–486 (2006).
- 496 46. Van Vuuren, D. P. *et al.* The representative concentration pathways: an overview. *Climatic*  
497 *Change* **109**, 5 (2011).



499

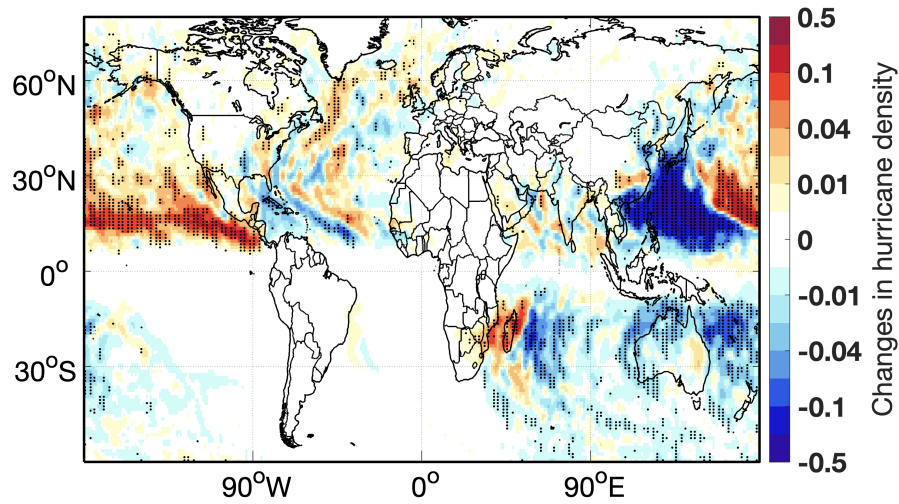
500 **Extended Data Fig. 1. Significant improvements in model’s reproduction skills.** Compared  
 501 with HadISST1-based simulations, accounting for groupwise corrections significantly ( $P < 0.05$ )  
 502 increases correlation ( $r^2$ ) and decreases RMSE with observed hurricane counts. Reproduction skills  
 503 are evaluated using 15-year running averaged counts from 1885 to 2011. The null distribution of  
 504 no improvement in reproduction skills (golden) is constructed using a Monte Carlo method that  
 505 makes random corrections to HadISST1-based simulations (see methods).





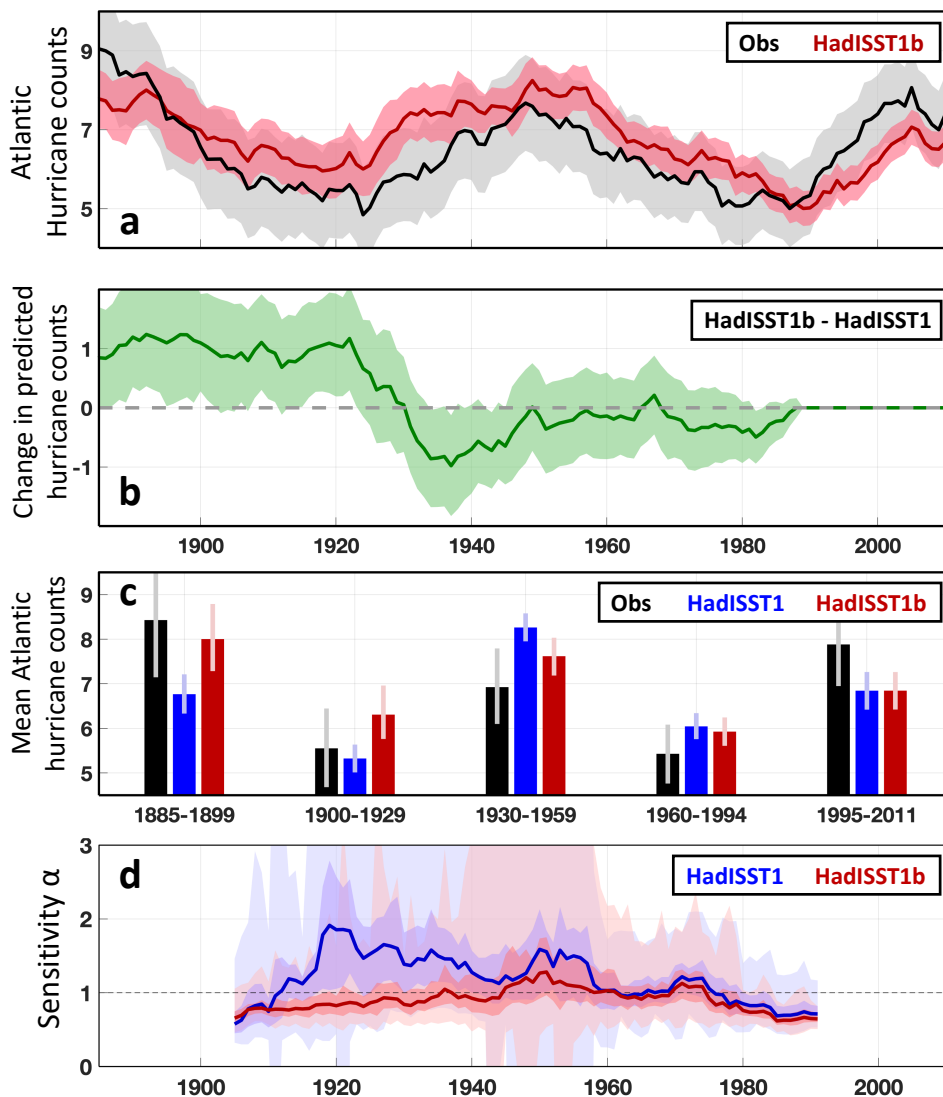
506

507 **Extended Data Fig. 2. RMSE between observed and ensemble-mean of simulated hurricane**  
 508 **counts.** RMSEs are calculated using 15-year moving averaged hurricane counts. The null distri-  
 509 bution (gray shading) is reconstructed using a Monte Carlo method by realizing only atmospheric  
 510 internal variability,  $\epsilon_i$ , errors associated with uncertain groupwise corrections,  $\frac{dF}{dT}\epsilon_T$ , and errors in  
 511 historical hurricane adjustment,  $\epsilon_o$ , following Eq. 1. Whereas the RMSE with HadISST1 (blue)  
 512 is higher than the 99th percentile of the null distribution, the RMSE with HadISST1b (red) is the  
 513 90th percentile and becomes consistent with the null distribution.



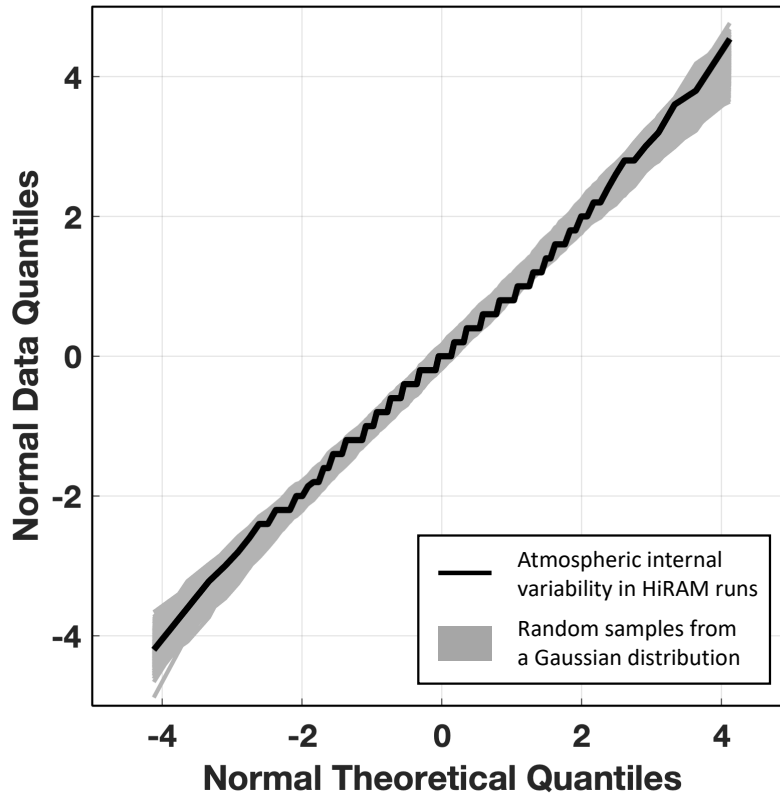
514

515 **Extended Data Fig. 3. Changes in hurricane track density in the RCP4.5 scenario.** Results  
 516 are based on time-slice simulations (see methods). Whereas the control simulation is prescribed  
 517 with 1982-2005 climatology in HadISST1, the RCP4.5 simulation implement increases in radia-  
 518 tive forcing in the RCP4.5 scenario<sup>46</sup> and 2081-2100 SST warming over and 17 CMIP5 coupled  
 519 models<sup>34</sup>. 50 years of data are collected for each simulation and dots denote significant changes in  
 520 hurricane density ( $P < 0.05$ , two-sample t-test,  $N = 50$ ).



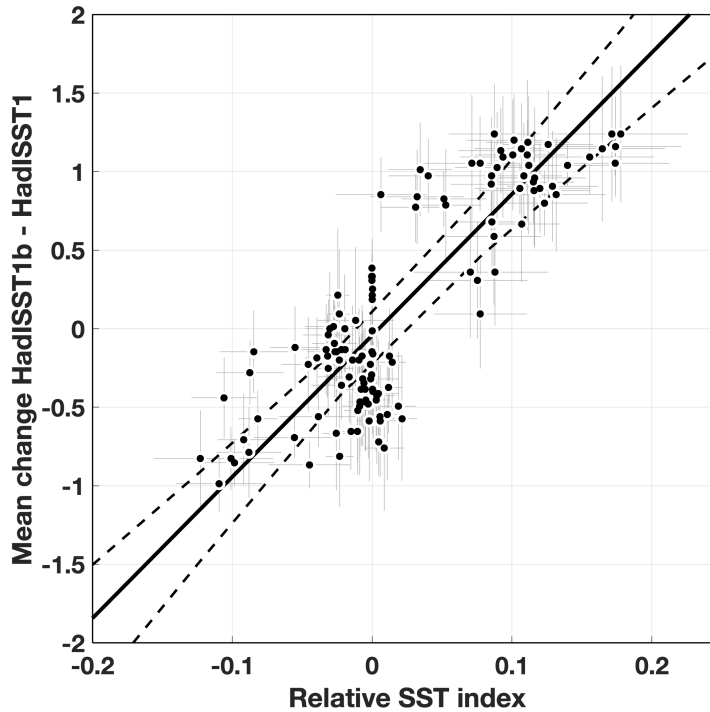
521

522 **Extended Data Fig. 4. Same as Fig. 1 but with SST corrections omitted after 1981.** To estimate  
 523 the sensitivity associated with turning off groupwise bucket SST corrections in the satellite era,  
 524 HadISST1b-based simulations since 1982 are replaced by simulations with HadISST1. Individual  
 525 panels are as Fig. 1b-d and Fig. 4a in the main text. Improvements in reproduction skill with  
 526 HadISST1b, together with a more stable relationship between Atlantic hurricane counts and SSTs,  
 527 are robust to splicing data in the satellite era.



528

529 **Extended Data Fig. 5. Atmospheric internal variability in HiRAM can be approximated**  
 530 **by a Gaussian distribution.** A quantile-quantile plot shows quantiles of atmospheric internal  
 531 variability in HiRAM simulations against quantiles of a Gaussian distribution that has zero mean  
 532 and a standard deviation of 1.97 (black). Atmospheric internal variability is quantified as the spread  
 533 of HiRAM members around the ensemble mean. Gray shading show the range of quantile-quantile  
 534 relationship wherein 1,000 random realizations of 1,480 samples are drawn from  $N(0, 1.97^2)$ .  
 535 1,480 is the total number of years in HadISST1 and HadISST1b HiRAM simulations and is the  
 536 sample size of the black curve.



537

538 **Extended Data Fig. 6. Changes in simulated Atlantic hurricane counts versus changes in the**  
 539 **relative SST index.** Changes in RSSTs (x-axis) are diagnosed from perturbed HadISST1b follow-  
 540 ing ref.<sup>14</sup> (also see methods). Changes in simulated hurricane counts when specifying HadISST1b  
 541 and HadISST1 in HIRAM simulations (green curve in Fig. 1c) are regressed against changes in  
 542 the relative SST index (black curve in Figure 3). A York regression is used that accounts for un-  
 543 certainties in hurricane counts (1 s.d. vertical bars) and RSST (1 s.d. horizontal bars). For display  
 544 purposes (and as shown in Fig. 1c) hurricane counts are smoothed using a 15-year running aver-  
 545 age but smoothing does not effect the York regression when the resulting smaller uncertainties are  
 546 accounted for.